Introduction

Periodontitis is an inflammatory disease caused by bacterial biofilms formed on the dental root surface. This disease can lead to irreversible destruction of the tooth-supporting tissues, including the alveolar bone, periodontal ligament, root cementum, and gingiva. Although conventional periodontal treatments based on mechanically removing the cause of disease shows some success in controlling inflammation and suppressing the progression of periodontitis, unfortunately these treatments rarely regenerate lost periodontal tissue or its functionality to any statistically or clinically significant level. Thus, periodontal regeneration therapy is required for successful periodontal treatment, which can be accomplished by re-formation of all components of the periodontium, including cementogenesis and osteogenesis.

Periodontal regeneration can be achieved, to some extent, by a variety of periodontal regenerative therapies, such as bone grafting, guided-tissue regeneration, application of enamel matrix derivatives, and cytokine therapies. However, the results are variable and the indication is limited to mild-to-moderate periodontal tissue defects. This may be because these therapies depend on the activity of somatic stem cells that exist within periodontal ligament tissue. As reported previously, an *in vitro* study revealed that aging can affect the proliferation and mineralized nodule formation of periodontal ligament cells and the number of stem cells within periodontal ligament tissue[1]. Moreover, progress of periodontitis not only destroys periodontal tissue but also deprives of existing somatic stem cells. Thus, it is important to use stem cells isolated from other tissues for periodontal regeneration, with a view to enhancing the outcome predictability and expanding the indication of regeneration therapy to severe periodontal defects[2].

Embryonic stem cells, induced pluripotent stem cells and somatic stem cells, are the three major stem cell sources. Owing to their safety and ethical profiles, somatic mesenchymal stem cells (MSCs) have been under intense investigation for clinical use in cell therapies. In terms of periodontal regeneration, transplantation of bone marrow-derived MSCs and periodontal ligament stem cells have been examined in preclinical[3, 4] and clinical studies[5, 6], highlighting their advantageous effects. However, difficulties associated with the isolation of these cells, including tissue harvesting, cell purifying from a heterogeneous cell population, and patient morbidity from associated harvesting pain, need to be overcome.

Adipose tissue-derived stem cells have been identified as a pluripotent cell population in adipose tissue, able to differentiate into several cell types[7]. These cells are also reported to secrete a variety of cytokines, including HGF, VEGF, TGF-β, IGF-1, and FGF-2, which are favorable factors for angiogenesis[8]. This cellular profile is thought to be important for the application of these cells in regenerative medicine. In addition, stem cells can be easily and safely obtained from adipose tissue without issues regarding tissue availability and ethics. To date, one group demonstrated that transplantation of adipose tissue-derived stem cells enhanced periodontal regeneration in the presence of platelet-rich plasma in rats and dogs[9, 10]. However, several issues remain to be addressed, including the effects solely from the transplanted cells and the safe and optimal scaffold material for these cells.

In this study, we isolated adipose tissue-derived multilineage progenitor cells (ADMPCs) from the greater omentum of beagle dogs and evaluated the cell characteristics. We then examined the effects of autologous transplantation of ADMPCs with fibrin gel into a furcation periodontitis model.

Materials and Methods

1)Experimental animals

Female beagle dogs, 50-56 months old, weighing 9-11 kg, were used and analyzed for experiments. All protocols were approved by the Institutional Animal Care and Use Committees of Osaka University Graduate School of Dentistry.

2)Isolation of ADMPCs

After beagle dogs were subcutaneously and intravenously anesthetized with 1 mL xylazine (Bayer Yakuhin, Ltd., Osaka, Japan) and 10 mg/kg pentobarbital (Kyoritsuseiyaku Co., Tokyo, Japan), respectively, the greater omentum was resected from each subject. ADMPCs were prepared as described previously[11]. Briefly, the resected greater omentum was minced and digested at 37℃ for 1 h in 0.075% collagenase (Wako Pure Chemical Industries, Osaka, Japan) in Hank's balanced salt solution. Digested tissue was diluted by adding Dulbecco's modified Eagle's medium high glucose (DMEM-HG; Gibco Life Technologies, CA, USA) with 20% fetal bovine serum (FBS; Sigma-Aldrich, St. Louis, MO, USA) and centrifuged at × 400 g

for 10 min. The cell pellet was suspended with DMEM-HG with 10% FBS and red blood cells were excluded using density gradient centrifugation with Histopaque (d=1.077 g/ml; Sigma). Cells were then filtered through a 40 μm cell strainer and cultured in DMEM-HG with 10% FBS at 37℃ for 24 h. Following incubation, cells were washed with phosphate buffered saline (PBS) and treated with 0.02% ethylenediaminetetraacetic acid (EDTA) solution (Nacalai Tesque, Kyoto, Japan). Floating cells, called ADMPCs, were collected and seeded onto a fibronectin-coated dish (BD Biosciences, San Jose, CA, USA) in 60% DMEM-low glucose (Gibco), 40% MCDB-201 medium (Sigma).

ADMPCs analyzed *in vitro* and *in vivo* were at passages 3 and 3.4, respectively.

3)Flow cytometric analysis

Isolated canine ADMPCs were characterized by flow cytometry. Single-cell suspensions were prepared by trypsinization with 0.05% trypsin / EDTA (Gibco) and incubated for 30 min at 4℃ with fluorescein isothiocyanate (FITC)-conjugated antibodies; mouse anti-canine CD29 (EXBIO, Praha, Czech Republic), rat anti-canine CD44 (eBioscience, San Diego, CA, USA,) and mouse anti-canine CD105 (BD Biosciences). Incubation with rat anti-canine CD90 (Thermo Scientific, Rockford, IL, USA) was followed by reaction with FITC-conjugated mouse anti-rat IgG antibody (BD Biosciences). Isotype-identical antibodies served as controls for each antigen. Data were collected with a FACSCalibur (BD Biosciences) and analyzed with CellQuest software.

4)Osteogenic and adipogenic differentiation procedure

For osteogenic differentiation, ADMPCs were cultured in 12-well plates until confluent and were then exposed to mineralization medium consisting of alpha modification of minimum essential medium; α-MEM supplemented with 10% FBS, 10 mM β-glycerophosphate, and 5 μM ascorbic acid, which was replaced every 3 days. Differentiation was examined by histochemical staining of calcified nodules with alizarin red S. Cell monolayers were washed twice with PBS and then fixed with dehydrated ethanol. After fixation, cell layers were stained with 1% alizarin red S (Wako) in 0.1% NH_4OH (pH 6.5) for 5 min, then washed with H_2O. For adipogenic differentiation, ADMPCs were cultured in 24-well plates until confluent and were then exposed to adipogenic-inducing medium consisting of α-MEM supplemented with 5% FBS, 500 μM 3-Isobutyl-1-methylanthine (Sigma), 10 μM Insulin (Sigma), 100 μM Indomethacin (Sigma), and 1 μM Dexamethasone (Sigma), which was replaced every 3 days. Differentiation was examined microscopically by observation of intracellular lipid droplets after staining with Oil Red O as follows; cell monolayers were fixed with 4% paraformaldehyde for 30 min, washed and stained with 0.16% Oil Red O for 20 min.

Table.1 Nucleotide sequences of primers used for PCR

Gene		Primer sequence
COL1A2	F	5'- GCACATGCCGAGACCTGAGA -3'
	R	5'- GCATCCATAGTGCATCCTTGGTTAG -3'
RUNX2	F	5'- TCATGGCGGGTAACGATGAA -3'
	R	5'- TCCGGCCCACAAATCTCAG -3'
PLAP-1	F	5'- TGCTCTGCCAAGCCATCATC -3'
	R	5'- GGTCGCCATCCATTTCATCTTC -3'
HPRT	F	5'- GGAGCATAATCCAAAGATGGTCAA -3'
	R	5'- TCAGGTTTATAGCCAACACTTCGAG -3'
LPL	F	5'- ACACATTCACAAGAGGGTCACC -3'
	R	5'- CTCTGCAATCACACGGATGGC -3'
Leptin	F	5'- CTATCTGTCCTGTGTTGAAGCTG -3'
	R	5'- GTGTGTGAAATGTCATTGATCCTG -3'

5)Reverse transcription-PCR

Total RNA was extracted from cultured cells using RNA-Bee (TEL-TEST, Inc., Friendwood, CA, USA) in accordance with the manufacturer's protocol. Purified total RNA was reverse transcribed using M-MLV (Invitrogen, Carlsbad, CA, USA) reverse transcriptase with random hexamers. Real-time PCR analysis was performed using Power SYBR Green PCR Master Mix and a 7300 Fast Real-Time PCR system (Applied Biosystems, Foster City, USA). The primer sequences used for PCR are listed in Table 1.

6)Surgical procedure and transplantation of ADMPCs

Extensive bone defects around the molar furcation area were surgically created in mandibular right and left premolars (P3 and P4) of beagle dogs, as shown in Fig.1. All surgeries were performed under pentobarbital anesthesia and local infiltrated anesthesia with 2% lidocaine hydrochloride and 1/80,000 epinephrine. After elevation of the mucoperiosteal flaps, the buccal bone was removed to create the bone defects (4 mm inferior and 3 mm horizontal). The

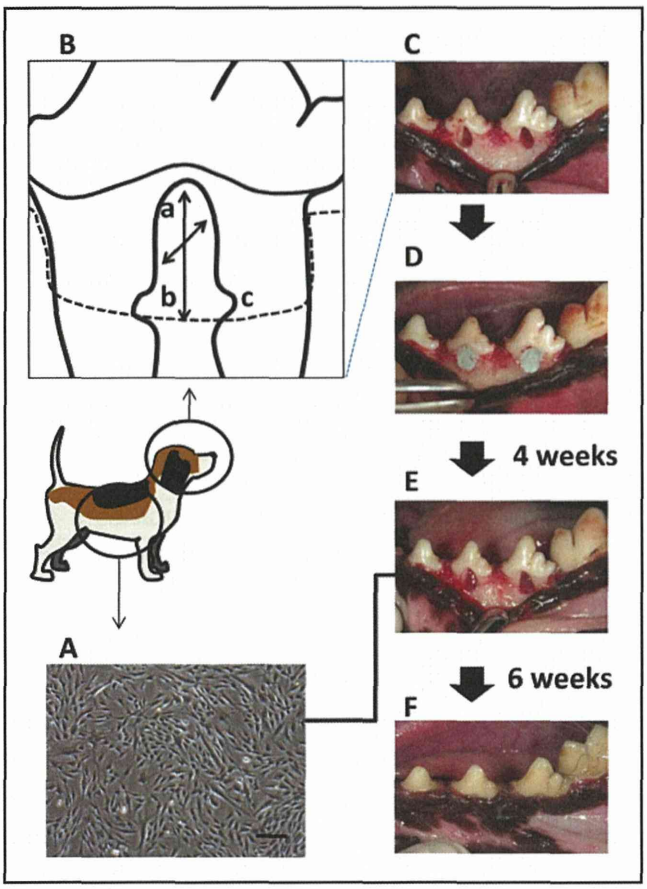

Fig.1 Schematics for ADMPC transplantation into the canine furcation periodontitis model

(A) Morphology of isolated ADMPCs. Scale bar = 200 μm. (B) Schematic illustration of the surgically created furcation defect. a: 3 mm horizontal, b: 4 mm inferior, c: horizontal groove. (C)-(F) Macroscopic view of the experimental sites. (C) Furcation bone defects were created in mandibular premolars. (D) Defects were filled with vinyl polysiloxane impression material. (E) 4 weeks after the procedure of (C) and (D), impression material and granulation tissue was removed and ADMPCs with fibrin gel or fibrin gel alone were transplanted into the defects. (F) Six weeks after the transplantation of ADMPCs.

exposed cementum of the teeth was removed using Gracey Curettes (Hu-Friedy. Co. Chicago, IL, USA) and tooth planing bars. Vinyl polysiloxane impression material (Putty type: GC Corporation, Tokyo, Japan) was placed in all furcation defects to initiate inflammation. The wounds were closed by suturing the flaps over the furcation defects and stitches were removed after 1 week. Four weeks after the first surgery, the full thickness flap was raised to expose the inflamed furcation and granulation tissue was removed. After root planing using a root planing bar, a horizontal groove on each root was made by a small round bar to indicate the base of the defect. The furcation defect of the right and left side was then filled with fibrin gel (Bolheal®; Teijin Pharma Limited, Tokyo, Japan) alone and the ADMPC-fibrin gel complex, respectively, and surgical closure was performed.

7)Micro-computed tomography (μCT) analysis

Under general anesthesia, beagle dogs were euthanized by exsanguination 6 weeks after transplantation. Tissues containing the transplanted region were extracted and fixed with 4% paraformaldehyde. Tissues were then scanned using a μCT apparatus (Scan Xmate-E090; Comscan Techno, Tokyo, Japan). Three-dimensional-CT (3D-CT) images were analyzed and quantified using image analysis software (TRI/3D-BON, Ratoc System Engineering, Tokyo, Japan).

8)Histological analysis

After μCT analysis, tissues were decalcified for 2 months in 10% formic acid, dehydrated, and embedded with paraffin. Serial sections (4 μm) were prepared in the mesial-distal plane. The mesio-distal plane in the center of the horizontal defect of each furcation involvement was then stained with Azan staining. Staining was performed as follows; deparaffinized sections were treated with dye mordant for 10 min and then stained with azocarmine G solution (Muto Pure Chemicals Co. Ltd., Tokyo, Japan.) for 30 min at 60℃. After differentiation in anilin-ethanol, reaction was stopped with 1% acetic ethanol. Then sections were treated with 5% phosphotungstic acid solution for 60 min, followed by anilin blue-orange G solution (Muto Pure Chemicals Co. Ltd.) for 30 min. And then dehydration and differentiation was performed with 100% ethanol. Histological measurements were performed using WinRoof® image analysis software (Mitani Corp., Tokyo, Japan). The new cementum formation rate was histomorphometrically calculated by dividing the length of newly formed cementum by the perimeter of intra-bony defect.

9)Statistical analysis

Data were expressed as the mean ± standard deviation (SD). Statistical analyses were performed by the Student's *t*-test. $p<0.05$ was considered statistically significant.

Results

1)Surface marker expression of ADMPCs

To assess MSC marker expression on ADMPCs isolated from the greater omentum, flow cytometric analysis was

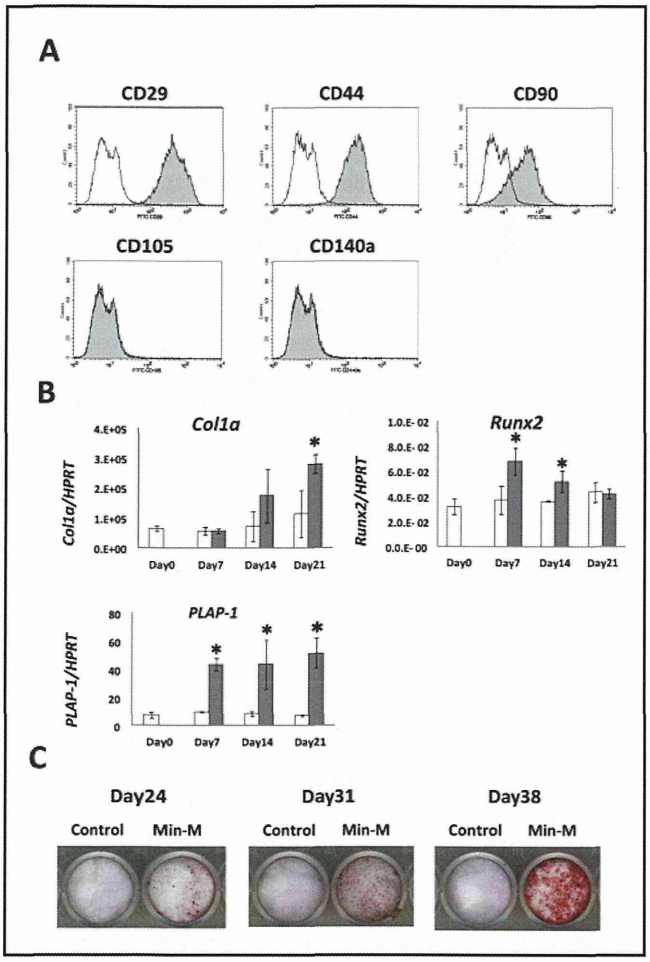

Fig.2 Characteristics of ADMPCs

(A) MSC surface marker expression on ADMPCs. Expression of each surface marker is shown with the shaded histogram. Staining with an isotype control antibody is shown with the black line. (B) *Type I collagen, Runx2*, and *PLAP-1* mRNA expression in ADMPCs cultured with (gray bar) or without (white bar) mineralization media (Min-M) for indicated days. Data are expressed as relative expression to *HPRT*. (C) Mineral deposition by ADMPCs cultured with or without Min-M. Cells were stained with alizarin red S on the indicated days.

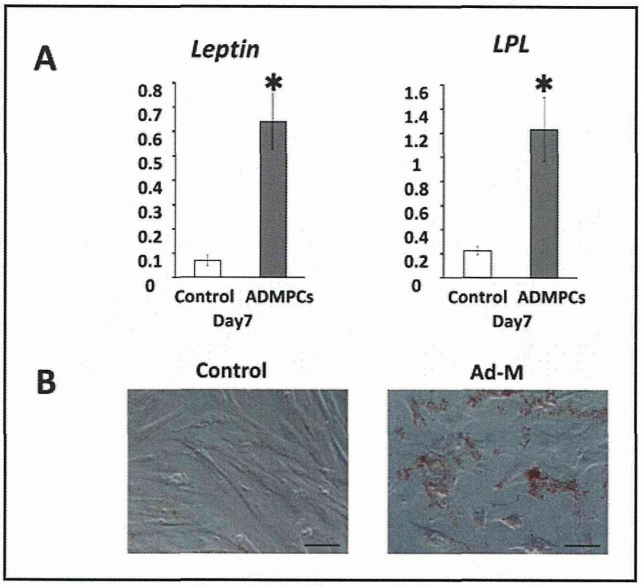

Fig.3 Adipogenic differentiation of ADMPCs

(A)Leptin and LPL mRNA expression in ADMPCs cultured with or without adipogenic-inducing media (Ad-M) for 7 days. Data are expressed as relative expression to *HPRT*. (B)Oil droplet formation by ADMPCs cultured with or without Ad-M. Cells were stained with Oil O red on day 28 of culture. Scale bar=100 μm Data are expressed as mean ± S.D. *p<0.05 compared with control.

performed. Isolated ADMPCs were found positive for the markers characteristic of canine mesenchymal stem cells, including CD29, CD44 and CD90, and were negative for CD105 and CD140a (Fig.2A), as previously reported[12].

2)Differentiation capability of ADMPCs

To examine the differentiation capability of ADMPCs, cells were cultured in mineralization media to induce osteoblastic differentiation. Gene expression of *type I collagen* and *Runx2* were significantly upregulated by induction (Fig.2B). Moreover, alizarin red S staining showed calcified nodule formation after 24 days of culture (Fig.2C). Notably, mRNA expression of *PLAP-1*, a specific molecule expressed in periodontal ligament tissue[13], was also increased (Fig.2B), suggesting not only osteoblastic capability but also potential to differentiate into periodontal ligament tissue. In addition, adipogenic differentiation was identified by gene expression of *leptin* and *lipoprotein lipase* (*LPL*) and oil droplet formation, after culture in an adipogenic-inducing medium (Fig.3). These results suggest the canine ADMPCs isolated from the greater omentum had multi-lineage differentiation capability.

3)Effects of ADMPC transplantation into the furcation periodontal defects

Inflamed furcation bony defects were artificially prepared and transplanted with either fibrin gel alone or autologous ADMPCs with fibrin gel. No severe inflammation or swelling was observed in any examined sites throughout the experimental period. Moreover, furcation areas in all experimental sites remained unexposed during the experimental period. As shown in Fig.4, μCT analysis revealed that transplantation of ADMPCs significantly enhanced alveolar bone regeneration compared with fibrin gel alone.

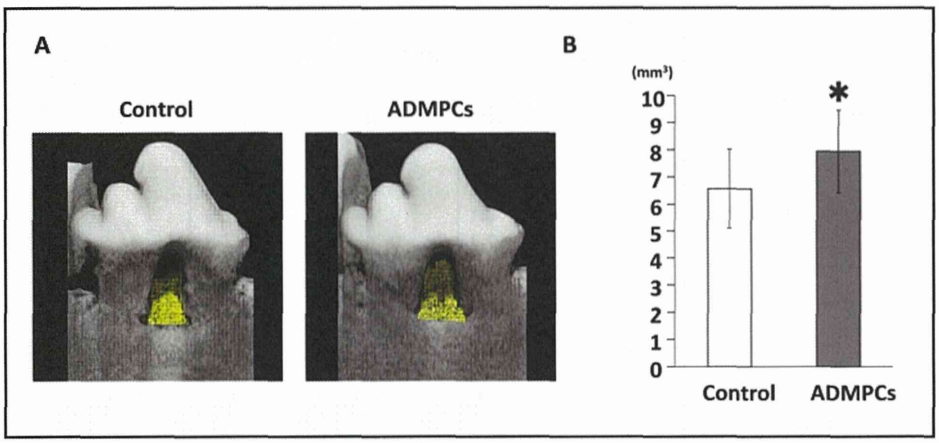

Fig.4 Quantitative analysis of new bone formation by μCT

(A) μCT reconstruction of the periodontal tissue defects transplanted with fibrin gel alone (control) or with ADMPCs + fibrin gel (ADMPCs). Six weeks after transplantation, mandibular tissues were harvested and scanned with μCT. Yellow area shows newly formed alveolar bone. (B) Quantitative analysis of reconstructed newly formed alveolar bone. (n=5) Data are expressed as mean ± S.D. *$p<0.05$ compared with control.

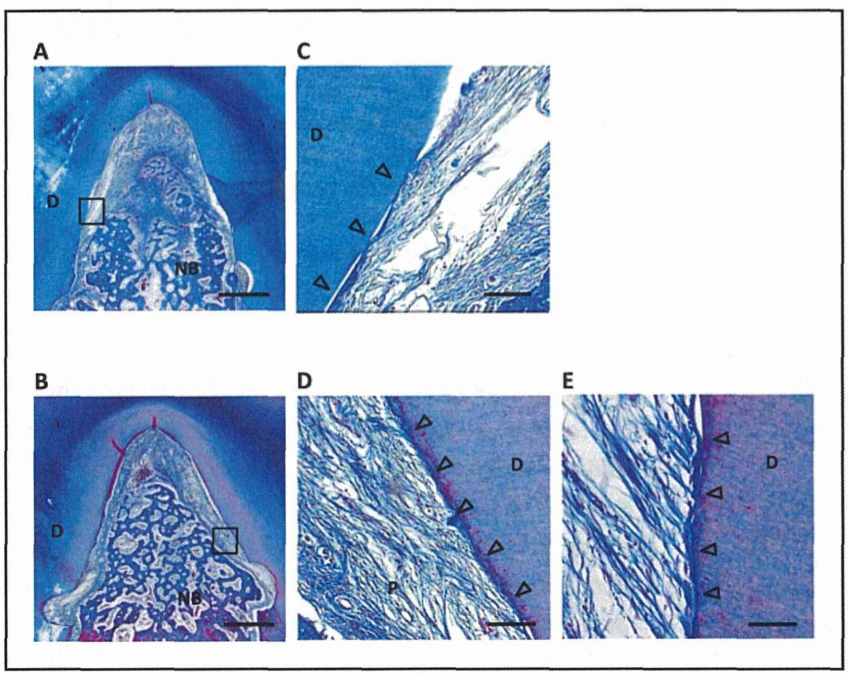

Fig.5 Histological analysis of periodontal tissue regeneration

Histological overview of furcation bone defects in the mesio-distal plane 6 weeks after transplantation. Histologic sections were stained with Azan. Representative image of fibrin gel applied site is shown in (A). Higher magnification of (A) is shown in (C). Representative image of fibrin gel + ADMPCs transplanted site is shown in (B). Higher magnification of (B) is shown in (D) and (E). Scale bar in (A) and (B)=1 mm. Scale bar in (C) and (D)=100 μm. Scale bar in (E)=50 μm. D: dentin, NB: new bone, P: periodontal ligament tissue, arrow head: newly formed cementum.

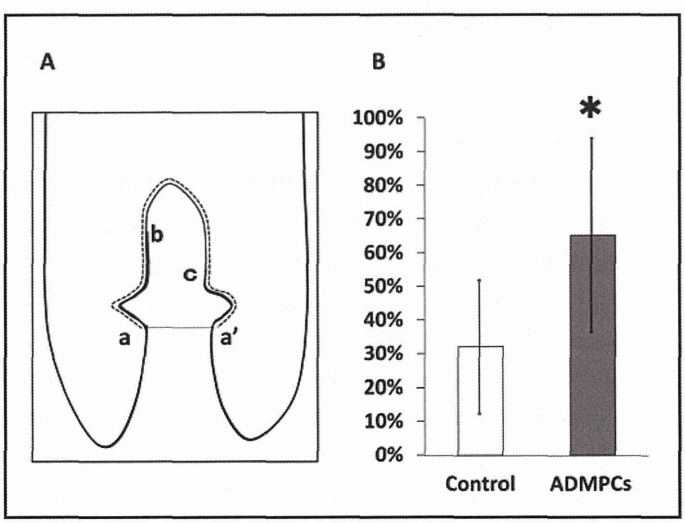

Fig.6 Histomorphometric analysis of new cementum formation

(A)Schematic drawing of histometric analysis of cementum formation 6 weeks after transplantation. Newly formed cementum rate=(a-b + a'-c)/a-a' x 100 (%) (B)Quantitative analysis of newly formed cementum rate. Data are expressed as mean ± S.D. *$p<0.05$ compared with control.

Histological observations of the furcation defects demonstrated periodontal regeneration, including new alveolar bone, and periodontal ligament and cementum formation with vertically inserted fibers in ADMPC transplanted sites (Fig.5). No undesirable healing occurred at ADMPC-transplanted sites, including root resorption or ankylosis. Histomorphometric analysis was performed and the new cementum formation rate was determined as described in Fig.6A. The new cementum formation rate following ADMPCs transplantation was significantly higher than those at control sites (Fig.6B).

Discussion

Current regenerative procedures to address periodontal tissue damaged following periodontitis have limitations in achieving complete and predicable regeneration. Based on tissue engineering, stem cell transplantation therapy is expected to overcome these issues. The present study demonstrates for the first time, the positive effects of ADMPCs, in the absence of extrinsic signaling molecules, in the treatment of periodontal defects in beagle dogs.

ADMPCs are readily extracted, can be expanded efficiently *in vitro*, and have the capacity to differentiate into multiple cell lineages, all of which are criteria in regenerative medicine. In fact, reports about the clinical application of ADMPCs have increased in a wide variety of fields. In most cases, ADMPCs are isolated from subcutaneous adipose tissue harvested by liposuction. Because there is insufficient adipose tissue under canine skin, the greater omentum was used as an ADMPC source in this study. Although it has been reported that ADMPCs from visceral fat have less proliferation and differentiation capacity compared with those from subcutaneous adipose tissue[14,15], ADMPCs used in this study significantly promoted periodontal regeneration. This finding promises greater impact of ADMPCs on future clinical trials, because subcutaneous adipose tissue is abundant and more readily accessible in humans.

During research into periodontal regeneration, a variety of animal models have been used. In this study, we employed the furcation periodontitis model in beagle dogs to evaluate the effects of ADMPC transplantation. Although we artificially induced inflammation in the defect site before ADMPC transplantation, the majority of periodontal regeneration preclinical studies have applied various biomaterials or cells just after surgical creation of defects. Our preclinical model is close to the clinical situation and our results enhance the utility value of ADMPCs for periodontal regeneration. In addition, we utilized clinical-grade fibrin gel (Bolheal®) as a scaffold for ADMPCs. Our preliminary study demonstrates that application of Bolheal® into periodontal defects does not impair the healing of periodontal tissue compared with sham procedure (data not shown).

ADMPCs possess the capacity to undergo osteogenic, adipogenic, chondrogenic, and myogenic differentiation. Notably, we showed not only the osteogenic and adipogenic differentiation of isolated ADMPCs, but also the induction of *PLAP-1* gene expression, a specific marker of periodontal ligament tissue (Fig.2), suggesting the differentiation capacity of these cells into periodontal ligament tissue. ADMPCs had not been induced to undergo differentiation prior to transplantation. It could therefore be hypothesized that transplanted ADMPCs home to and differentiate into specialized cells in the transplanted sites adequately. Although this hypothesis needs to be demonstrated in future studies, this is supported by previous studies in which transplanted stem cells in periodontal bone defects, at least in part, differentiated into cementoblasts, osteoblasts, osteocytes and fibroblasts in regenerated periodontal tissue[10, 16].

Recent work, on the other hand, demonstrates that the mechanism by which stem cells participate in tissue repair and regeneration is related to their trophic factors[17, 18]. In fact, our pilot studies show that ADMPCs secrete a number of growth factors, and conditioned medium from ADMPCs can stimulate differentiation of periodontal ligament cells to hard tissue-forming cells (data not shown). These results suggest a possible mechanism that transplanted ADMPCs secrete a number of factors, which can activate the tissue surrounding the periodontal defect, resulting in promotion of the regeneration process.

In conclusion, transplantation of ADMPCs with fibrin gel into periodontal defects has a positive effect on periodontal regeneration. Further investigations will be required to reveal the molecular mechanisms of this therapy and the true potential of this procedure, including the extent of periodontal destruction that can be rescued. It also needs to be determined which signaling molecules or scaffold materials or a combination of these give ADMPCs the optimal environment to regenerate periodontal tissue. As a consequence, we are confident that periodontal regeneration

therapy, achieving the ultimate goal of complete periodontal tissue regeneration following periodontal disease, will be developed.

Source of Funding and Conflict of Interest

This study was supported by a Grant-in-Aid for Scientific Research from the Ministry of Education, Culture, Sports, Science and Technology (Nos. 23390452, 24792326, and 23249086) and a Grant-in-Aid from the Ministry of Health, Labour and Welfare of Japan. The authors declare no conflicts of interest.

References

1) Zheng W, Wang S, Ma D, Tang L, Duan Y, Jin Y: Loss of proliferation and differentiation capacity of aged human periodontal ligament stem cells and rejuvenation by exposure to the young extrinsic environment. Tissue Eng Part A. 2009; 15: 2363-2371.
2) Hynes K, Menicanin D, Gronthos S, Bartold PM: Clinical utility of stem cells for periodontal regeneration. Periodontol 2000. 2012; 59: 203-227.
3) Kawaguchi H, Hirachi A, Hasegawa N, Iwata T, Hamaguchi H, Shiba H, et al: Enhancement of periodontal tissue regeneration by transplantation of bone marrow mesenchymal stem cells. J Periodontol. 2004; 75: 1281-1287.
4) Iwata T, Yamato M, Tsuchioka H, Takagi R, Mukobata S, Washio K, et al: Periodontal regeneration with multilayered periodontal ligament-derived cell sheets in a canine model. Biomaterials. 2009; 30: 2716-2723.
5) Yamada Y, Ueda M, Hibi H, Baba S: A novel approach to periodontal tissue regeneration with mesenchymal stem cells and platelet-rich plasma using tissue engineering technology: A clinical case report. Int J Periodontics Restorative Dent. 2006; 26: 363-369.
6) Feng F, Akiyama K, Liu Y, Yamaza T, Wang TM, Chen JH, et al: Utility of PDL progenitors for in vivo tissue regeneration: a report of 3 cases. Oral Dis. 2010; 16: 20-28.
7) Zuk PA, Zhu M, Mizuno H, Huang J, Futrell JW, Katz AJ, et al: Multilineage cells from human adipose tissue: implications for cell-based therapies. Tissue Eng. 2001; 7: 211-228.
8) Gimble JM, Katz AJ, Bunnell BA: Adipose-derived stem cells for regenerative medicine. Circ Res. 2007; 100: 1249-1260.
9) Tobita M, Uysal CA, Guo X, Hyakusoku H, Mizuno H: Periodontal tissue regeneration by combined implantation of adipose tissue-derived stem cells and platelet-rich plasma in a canine model. Cytotherapy. 2013; 15: 1517-1526.
10) Tobita M, Uysal AC, Ogawa R, Hyakusoku H, Mizuno H: Periodontal tissue regeneration with adipose-derived stem cells. Tissue Eng Part A. 2008; 14: 945-953.
11) Komoda H, Okura H, Lee CM, Sougawa N, Iwayama T, Hashikawa T, et al: Reduction of N-glycolylneuraminic acid xenoantigen on human adipose tissue-derived stromal cells/mesenchymal stem cells leads to safer and more useful cell sources for various stem cell therapies. Tissue Eng Part A. 2010; 16: 1143-1155.
12) Vieira NM, Brandalise V, Zucconi E, Secco M, Strauss BE, Zatz M: Isolation, characterization, and differentiation potential of canine adipose-derived stem cells. Cell Transplant. 2010; 19: 279-289.
13) Yamada S, Murakami S, Matoba R, Ozawa Y, Yokokoji T, Nakahira Y, et al: Expression profile of active genes in human periodontal ligament and isolation of PLAP-1, a novel SLRP family gene. Gene. 2001; 275: 279-286.
14) Baglioni S, Cantini G, Poli G, Francalanci M, Squecco R, Di Franco A, et al: Functional differences in visceral and subcutaneous fat pads originate from differences in the adipose stem cell. PLoS One. 2012; 7: e36569.
15) Toyoda M, Matsubara Y, Lin K, Sugimachi K, Furue M: Characterization and comparison of adipose tissue-derived cells from human subcutaneous and omental adipose tissues. Cell Biochem Funct. 2009; 27: 440-447.
16) Hasegawa N, Kawaguchi H, Hirachi A, Takeda K, Mizuno N, Nishimura M, et al: Behavior of transplanted bone marrow-derived mesenchymal stem cells in periodontal defects. J Periodontol. 2006; 77: 1003-1007.
17) Jayaraman P, Nathan P, Vasanthan P, Musa S, Govindasamy V: Stem cells conditioned medium: a new approach to skin wound healing management. Cell Biol Int. 2013; 37: 1122-1128.
18) Osugi M, Katagiri W, Yoshimi R, Inukai T, Hibi H, Ueda M: Conditioned media from mesenchymal stem cells enhanced bone regeneration in rat calvarial bone defects. Tissue Eng Part A. 2012; 18: 1479-1489.

BNIP3 Plays Crucial Roles in the Differentiation and Maintenance of Epidermal Keratinocytes

Mariko Moriyama[1,2,4], Hiroyuki Moriyama[1,4], Junki Uda[1], Akifumi Matsuyama[2], Masatake Osawa[3] and Takao Hayakawa[1]

Transcriptome analysis of the epidermis of *Hes1*$^{-/-}$ mouse revealed the direct relationship between Hes1 (hairy and enhancer of split-1) and BNIP3 (BCL2 and adenovirus E1B 19-kDa-interacting protein 3), a potent inducer of autophagy. Keratinocyte differentiation is going along with activation of lysosomal enzymes and organelle clearance, expecting the contribution of autophagy in this process. We found that BNIP3 was expressed in the suprabasal layer of the epidermis, where autophagosome formation is normally observed. Forced expression of BNIP3 in human primary epidermal keratinocytes (HPEKs) resulted in autophagy induction and keratinocyte differentiation, whereas knockdown of BNIP3 had the opposite effect. Intriguingly, addition of an autophagy inhibitor significantly suppressed the BNIP3-stimulated differentiation of keratinocytes, suggesting that BNIP3 plays a crucial role in keratinocyte differentiation by inducing autophagy. Furthermore, the number of dead cells increased in the human epidermal equivalent of BNIP3 knockdown keratinocytes, which suggests that BNIP3 is important for maintenance of skin epidermis. Interestingly, although UVB irradiation stimulated BNIP3 expression and cleavage of caspase3, suppression of UVB-induced BNIP3 expression led to further increase in cleaved caspase3 levels. This suggests that BNIP3 has a protective effect against UVB-induced apoptosis in keratinocytes. Overall, our data provide valuable insights into the role of BNIP3 in the differentiation and maintenance of epidermal keratinocytes.

Journal of Investigative Dermatology (2014) **134,** 1627–1635; doi:10.1038/jid.2014.11; published online 6 February 2014

INTRODUCTION

The skin epidermis is a stratified epithelium. Stratification is a key process of epidermal development. During epidermal development, the single layer of basal cells undergoes asymmetric cell division to stratify, and produce committed suprabasal cells on the basal layer. These suprabasal cells are still immature and sustain several rounds of cell divisions to form fully stratified epithelia. Recent studies have identified numerous molecules involved in epidermal development, although how these molecules coordinate to induce proper stratification of the epidermis remains to be elucidated. Previously, by integrating both loss- and gain-of-function studies of Notch receptors and their downstream target Hes1 (hairy and enhancer of split-1), we demonstrated the multiple roles of Notch signaling in the regulation of suprabasal cells (Moriyama *et al.*, 2008). Notch signaling induces differentiation of suprabasal cells in a Hes1-independent manner, whereas Hes1 is required for maintenance of the immature status of suprabasal cells by preventing premature differentiation. In light of the critical role of Hes1 in the maintenance of spinous cells, exploration of the molecular targets of Hes1 in spinous layer cells may lead to the discovery of the molecules required for differentiation of spinous layer cells to granular layer cells. Because Hes1 is thought to be a transcriptional repressor (Ohtsuka *et al.*, 1999), loss of Hes1 is expected to cause aberrant upregulation of genes that are normally repressed in spinous layer cells. To identify these genes, we previously conducted comparative global transcript analysis using microarrays and found several candidates that may play a crucial role in regulating epidermal development (Moriyama *et al.*, 2008). One of the genes that was highly expressed was *BNIP3* (*BCL2 and adenovirus E1B 19-kDa-interacting protein 3*), an atypical pro-apoptotic BH3-only protein that induces cell death and autophagy (Zhang and Ney, 2009).

The molecular mechanism through which BNIP3 induces cell death is not well understood; however, it has been reported that BNIP3 protein is induced by hypoxia in some tumor cells and that the kinetics of this induction correlate with cell death (Sowter *et al.*, 2001). In contrast,

[1]*Pharmaceutical Research and Technology Institute, Kinki University, Higashi-Osaka, Osaka, Japan;* [2]*Platform for Realization of Regenerative Medicine, Foundation for Biomedical Research and Innovation, Kobe, Hyogo, Japan and* [3]*Division of Regeneration Technology, Gifu University School of Medicine, Gifu, Gifu, Japan*

[4]*These authors contributed equally to this work.*

Correspondence: Mariko Moriyama, Pharmaceutical Research and Technology Institute, Kinki University, Higashi-Osaka, Osaka 577-8502, Japan. E-mail: mariko@phar.kindai.ac.jp

Abbreviations: 3-MA, 3-methyladenine; BNIP3, BCL2 and adenovirus E1B 19-kDa-interacting protein 3; ChIP, chromatin immunoprecipitation; Hes1, hairy and enhancer of split-1; HPEK, human primary epidermal keratinocyte; Q-PCR, quantitative PCR

Received 18 July 2013; revised 10 December 2013; accepted 18 December 2013; accepted article preview online 8 January 2014; published online 6 February 2014

BNIP3-induced autophagy has been shown to protect HL-1 myocytes from cell death in an ischemia–reperfusion model (Hamacher-Brady *et al.*, 2007). Induction of autophagy by BNIP3 has a protective effect in some conditions, whereas in others it is associated with autophagic cell death. Recent evidence also suggests that BNIP3, through autophagy, is also required for the differentiation of chondrocytes under hypoxic conditions (Zhao *et al.*, 2012).

Autophagy was initially described based on its ultrastructural features of the double-membraned structures that surrounded the cytoplasm and organelles in cells, known as autophagosomes (Mizushima *et al.*, 2010). To date, only microtubule-associated protein light chain 3 (LC3), a mammalian homolog of yeast Atg8, is known to be expressed in autophagosomes and, therefore, it serves as a widely used marker for autophagosomes (Kabeya *et al.*, 2000; Mizushima *et al.*, 2004). Autophagy is an evolutionarily conserved catabolic program that is activated in response to starvation or changing nutrient conditions. Recently, autophagy was shown to be involved in differentiation of multiple cell types, including erythrocytes, lymphocytes, adipocyte, neuron, and chondrocyte (Srinivas *et al.*, 2009; Mizushima and Levine, 2010).

Epidermal cornification, the process of terminal keratinocyte differentiation, requires programmed cell death in a similar but different pathway from apoptosis (Lippens *et al.*, 2005). Cornification is also accompanied by activation of lysosomal enzymes and organelle clearance. Moreover, some researchers have reported that autophagy may play a role in epidermal differentiation (Haruna *et al.*, 2008; Aymard *et al.*, 2011; Chatterjea *et al.*, 2011). Therefore, it is likely that BNIP3 is involved in cornification through cell death or autophagy.

In this study, transcriptome analysis of *Hes1*$^{-/-}$ mouse epidermis revealed that Hes1 could directly suppress BNIP3 expression in epidermal keratinocytes. We also found that BNIP3 was expressed in the suprabasal layer of the human skin epidermis, where autophagosome formation was observed. BNIP3 was also sufficient to promote cornification through induction of autophagy. Finally, we found that BNIP3 had a protective effect against UVB-induced apoptosis in keratinocytes *in vitro*. Our data thus indicate that BNIP3, an inducer of autophagy, is involved in the terminal differentiation and maintenance of epidermal keratinocytes.

RESULTS

Hes1 directly represses BNIP3 expression in epidermal cells and keratinocytes

We previously performed a microarray analysis with epidermal RNAs isolated from wild-type and *Hes1*$^{-/-}$ mice (Moriyama *et al.*, 2008) and found that BNIP3 was preferentially overexpressed in *Hes1*$^{-/-}$ epidermis. The upregulation of *Bnip3* in the *Hes1*$^{-/-}$ epidermis was confirmed by quantitative PCR (Q-PCR) and immunofluorescent staining (Figure 1a and b). As Hes1 is thought to be a transcriptional repressor (Ishibashi *et al.*, 1994), it might play a repressive role in the regulation of BNIP3 expression. In accordance with this hypothesis, BNIP3 expression in *Hes1*$^{-/-}$ epidermis at embryonic day 15.5 was observed in the suprabasal layers (Figure 1b), where Hes1 has been reported to be expressed in wild-type epidermis at the same age (Blanpain *et al.*, 2006; Moriyama *et al.*, 2008). To confirm whether Hes1 suppresses BNIP3 expression, an adenoviral vector expressing Hes1 was used to infect human primary epidermal keratinocytes (HPEKs) and, subsequently, the expression level of BNIP3 was quantified by Q-PCR and western blot analysis. The BNIP3 protein was detected as multiple bands between 22 and 30 kD as previously reported (Vengellur and LaPres, 2004; Walls *et al.*, 2009; Mellor *et al.*, 2010; Sassone *et al.*, 2010). We found that Hes1 induced a substantial reduction of BNIP3 expression in HPEKs at the mRNA and protein levels (Figure 1c and d), demonstrating that Hes1 is involved in the repression of BNIP3. To determine whether Hes1 directly regulates *BNIP3* expression, we performed chromatin immunoprecipitation (ChIP) assays. We identified at least 5 Hes1 consensus binding sites 1 kb upstream of the transcription initiation site of the human *BNIP3* gene, and subsequent Q-PCR analysis revealed that a DNA fragment located at -247 to -87 was slightly amplified from crosslinked chromatin isolated by Hes1 immunoprecipitation (Figure 1e). We also found an additional site between -212 and $+22$ that was strongly amplified. These data clearly show that Hes1 specifically binds to the promoter region of *BNIP3* and directly suppresses its expression.

BNIP3 is expressed in the granular layer of the epidermis, where autophagosome formation is observed

To determine the BNIP3 expression profile in the epidermis, we performed immunofluorescent staining in human skin epidermal equivalent. BNIP3 was expressed in the granular layer of epidermal equivalent 18 days (Figure 2a and b) or 24 days (Figure 2c and d) after exposure at the air–liquid interface. BNIP3 expression in the granular layer was also observed in the normal human skin epidermis (Figure 2g and h). Recent reports show that BNIP3 is expressed in mitochondria and that it induces autophagy (Quinsay *et al.*, 2010). In addition, some researchers have reported that autophagy may play a role in epidermal differentiation (Haruna *et al.*, 2008; Aymard *et al.*, 2011; Chatterjea *et al.*, 2011). We therefore investigated whether autophagy occurred in the epidermis, especially in the granular layers. To quantitate the level of autophagy, cytosol to membrane translocation of the autophagy marker EGFP-LC3 (Kabeya *et al.*, 2000) was monitored in a human skin equivalent model (Mizushima *et al.*, 2004). When autophagy is active, autophagosomes containing EGFP-LC3 are visible as fluorescent puncta (Kabeya *et al.*, 2000). As expected, EGFP-LC3 puncta were observed in the granular layers of the epidermal equivalent (Figure 2e). Moreover, endogenous LC3 dots were observed in the granular layers of normal human skin epidermis (Figure 2f). These data suggested that BNIP3 might be involved in the induction of autophagy in the granular layer of the epidermis.

BNIP3 is required for terminal differentiation of keratinocyte by induction of autophagy *in vitro*

To investigate the involvement of BNIP3 in the induction of autophagy, we transduced HPEKs stably expressing EGFP-LC3

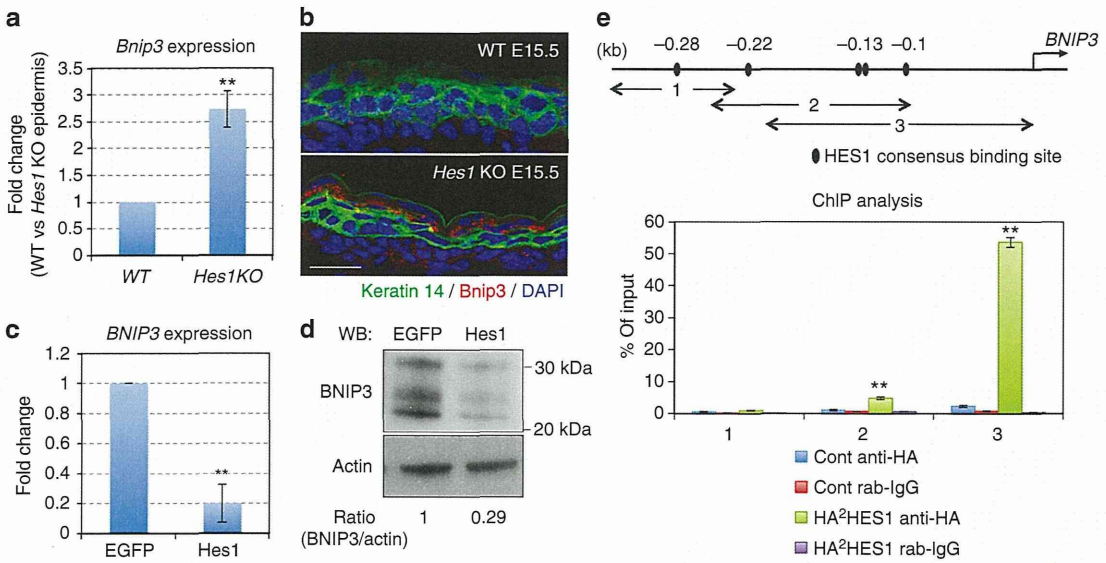

Figure 1. BNIP3 (BCL2 and adenovirus E1B 19-kDa-interacting protein 3) is directly suppressed by HES1(hairy and enhancer of split-1). (**a**) Quantitative PCR (Q-PCR) analysis of *Bnip3* expression in dorsal skin epidermis from either wild-type (WT) or *Hes1* knockout (KO) embryo (embryonic day 14.5 (E14.5)). (**b**) Immunofluorescent analysis of Bnip3 expression in dorsal skin epidermis from either WT or *Hes1* KO embryo (E15.5). Keratin 14 staining is shown in green and Bnip3 staining is shown in red. The blue signals indicate nuclear staining. Scale bars = 20 μm. (**c**) Q-PCR and (**d**) western blot analysis of BNIP3 expression in human primary epidermal keratinocyte (HPEK) cells infected with adenoviruses expressing enhanced green fluorescent protein (EGFP) or Hes1. (**c**) Each expression value was calculated with the ΔΔCt method using *UBE2D2* as an internal control. (**d**) Numbers below blots indicate relative band intensities as determined by ImageJ software. (**e**) Specific binding of Hes1 to the *BNIP3* promoter. HPEK cells were infected with adenoviral constructs expressing hemagglutinin (HA)-tagged Hes1, and processed for chromatin immunoprecipitation (ChIP) with an anti-HA antibody and normal rabbit immunoglobulin G (Cont rab-IgG) as a nonimmune control. Q-PCR amplification of the region of the *BNIP3* gene described in the indicated map (upper panel; nucleotides −360 to −244 (1); nucleotides −247 to −87 (2); −212 to +22 (3)) was also performed. The amount of precipitated DNA was calculated relative to the total input chromatin. All the data represent the average of three independent experiments ± SD. $^{**}P<0.01$.

with a BNIP3 adenoviral vector. BNIP3 expression was found to be sufficient to trigger the formation of EGFP-LC3 puncta that was significantly reduced by addition of 3-methyladenine (3-MA), an inhibitor of autophagy (Figure 3a and b). On the other hand, BNIP3 knockdown markedly decreased the punctuate distribution of EGFP-LC3 in differentiated HPEKs (Figure 3c and d). Furthermore, flow cytometry analysis using a green fluorescent probe used to specifically detect autophagy (Cyto-ID autophagy detection dye) (Chan *et al.*, 2012) also showed that BNIP3 was required for the autophagy induction (Figure 3c and f). These data indicate that BNIP3 is involved in the induction of autophagy in HPEKs. Intriguingly, these data also confirm the previous finding that autophagosome induction is accompanied by keratinocyte differentiation (Haruna *et al.*, 2008). We observed that the number of mitochondria was decreased in the granular layers, where BNIP3 expression and autophagosome formation was observed (Figure 4a). In addition, mitochondria were significantly decreased in the differentiated HPEKs *in vitro* (Figure 4b). Colocalizations of mitochondria and EGFP-LC3 dot were observed only in the differentiating keratinocytes (Figure 4c), suggesting the contribution of autophagy in the decrease of mitochondria. BNIP3 expression was also correlated with decreased mitochondria in HPEKs, whereas addition of 3-MA restored mitochondrial numbers (Figure 4d). Furthermore, we also observed colocalization of mitochondria and EGFP-LC3 dot in BNIP3-overexpressing HPEKs (Figure 4e). These data indicated that mitochondria were removed by BNIP3-induced autophagy. Next, we investigated the involvement of BNIP3 in the differentiation of epidermal keratinocytes. Western blot analysis and immunofluorescent staining revealed that BNIP3 expression increased during differentiation (Figure 5a and b). Knockdown of BNIP3 significantly suppressed keratinocyte differentiation when the cells were treated with differentiation medium (Figure 5c and d), indicating that BNIP3 is required for terminal differentiation of keratinocyte. On the other hand, forced expression of BNIP3 in HPEKs markedly stimulated loricrin expression (Figure 5e and f). To determine whether BNIP3-dependent keratinocyte differentiation was induced by autophagy, 3-MA was added to the cells transduced with BNIP3. As shown in Figure 5e and f, 3-MA notably abolished the keratinocyte differentiation induced by BNIP3, suggesting that BNIP3 is required for terminal differentiation of keratinocyte by induction of autophagy.

BNIP3 maintains epidermal keratinocytes

To further determine the roles of BNIP3 in epidermal differentiation, the human skin epidermal equivalent was reconstituted from HPEKs stably expressing a BNIP3 RNA interference (RNAi). Unfortunately, we did not observe drastic differentiation defects; however, we unexpectedly discovered